PHYSICAL REVIEW B **83**, 180503(R) (2011)

Spin-glass behavior of semiconducting $K_xFe_{2-y}S_2$

Hechang Lei (雷 和 畅), Milinda Abeykoon, Emil S. Bozin, and C. Petrovic
Condensed Matter Physics and Materials Science Department, Brookhaven National Laboratory, Upton, New York 11973, USA
(Received 28 January 2011; revised manuscript received 19 March 2011; published 16 May 2011)

We report the discovery of $K_xFe_{2-y}S_2$ single crystals, isostructural to $K_xFe_{2-y}Se_2$ superconductors. The sulfide compound is a small gap semiconductor and shows spin-glass behavior below 32 K. Our results indicate that stoichiometry, defects, and the local environment of FeCh (Ch = S,Se) tetrahedra have important effects on the physical properties of isostructural and isoelectronic $K_xFe_{2-y}Ch_2$ compounds.

DOI: 10.1103/PhysRevB.83.180503 PACS number(s): 74.70.Xa, 74.70.Ad, 75.50.Lk, 74.72.Cj

Iron-based materials have been the focus of exploratory search for new superconductors since the discovery of $LaFeAsO_{1-x}F_x$ with a transition temperature T_c up to 26 K.[1] Several superconducting families were discovered soon after *R*FePnO (*R* = rare earth; Pn = P or As, FePn-1111 type),[2–4] including α-PbO-type FeCh (Ch = S,Se,Te; FeCh-11 type) materials that do not have any crystallographic layers in between puckered FeCh slabs.[4] FeCh-11-type materials share a square-planar lattice of Fe with a tetrahedral coordination and Fermi surface topology similar to other iron-based superconductors.[5] Under external pressure,[6,7] T_c can be increased from 8 to 37 K and dT_c/dP can reach 9.1 K/GPa, the highest in all iron-based superconductors.[7] The empirical rule proposed by Mizuguchi *et al.* proposes that the critical temperature is closely correlated with the anion height between Fe and Ch layers. There is an optimal distance around 0.138 nm with a maximum transition temperature $T_c \simeq 55$ K.[8]

Intercalation can change the local environment of the FeSe tetrahedron and introduce extra carriers. The intercalation could also decrease the dimensionality of the conducting bands. This is favorable for superconductivity since the presence of low-energy electronic collective modes in layered conductors helps to screen Coulomb interaction.[9] This is seen in iron-based superconductors: T_c increases from FeCh-11 type to FePn-1111 type. Very recently the superconducting T_c was enhanced in iron selenide material to about 30 K not by external pressure but by inserting K, Rb, Cs, and Tl between the FeSe layers (AFeSe-122 type), thus changing the crystal structure around the FeCh tetrahedra.[10–13] Similar to pressure effects, the intercalation using elements with +1 valence decreases the Se height toward the optimum value.[12] The expanded FeSe interlayer distances could also contribute to reducing the dimensionality of the conducting bands and magnetic interactions. On the other hand, the insulating-superconducting transition can be induced in $(Tl_{1-x}K_x)Fe_{2-y}Se_2$ by tuning the Fe stoichiometry and implying that the superconductivity is in the proximity of an antiferromagnetic Mott-insulating state.[13] Thus, exploring new oxychalcogenide and chalcogenide compounds containing similar FeCh layers would be instructive.

In this Rapid Communication, we report the discovery of $K_xFe_{2-y}S_2$ single crystals isostructural to 122 iron selenide superconductors. The structure analysis indicates that the anion height might not be essential for superconductivity. The resistivity and magnetic measurements suggest a spin-glass (SG) semiconductor ground state similar to that of the $TlFe_{2-x}Se_2$ with high Fe deficiency, even though the anion heights are close to values found in iron-based superconductors with T_c above 20 K.[13,14]

Single crystals of $K_xFe_{2-y}S_2$ were grown via the self-flux method[15] with nominal composition K:Fe:S = 0.8:2:2. Prereacted FeS and K pieces were added into the alumina crucible with a partial pressure of argon gas. The quartz tubes were heated to 1030°C, kept at this temperature for 3 h, then cooled to 730°C. Platelike crystals up to $10 \times 10 \times 3$ mm^3 can be grown. Powder x-ray diffraction (XRD) data were collected at 300 K using 0.3184-Å wavelength radiation (38.94 keV) at the X7B beamline of the National Synchrotron Light Source. The average stoichiometry was determined by energy-dispersive x-ray spectroscopy (EDX). Electrical transport, heat capacity, and magnetization measurements were carried out in Quantum Design PPMS-9 and MPMS-XL5.

Figure 1(a) shows powder XRD data at room temperature and structural refinements on $K_xFe_{2-y}S_2$ using General Structure Analysis System (GSAS).[16,17] A model possessing tetragonal $ThCr_2Si_2$ structure and space group I4/mmm failed to explain the observed diffraction pattern due to the clear appearance of (110) and other superlattice reflections indicating symmetry lowering to I4/m. Data were successfully explained to within I4/m symmetry, incorporating the Fe vacancy order site, with lattice parameters $a = 8.3984(5)$ Å and $c = 13.5988(11)$ Å, which are appreciably smaller than those observed in the selenium counterpart.[10] The c axis is particularly reduced due to the smaller ionic size of S^{2-} when compared to Se^{2-}. The ordered Fe vacancy is the same as in $K_xFe_{2-y}Se_2$.[18] This may imply a similar origin of magnetic behavior for both compounds. Atomic positions with refined parameters are listed in Table I. Refinements yield that K1, K2, and Fe1 positions are partially occupied, while Fe2 positions are almost fully occupied. It should be noted that, when K1 and Fe1 positions are fully unoccupied while K2 and Fe2 are fully occupied, the corresponding chemical formula is $K_{0.8}Fe_{1.6}S_2$ and the Fe vacancy is completely ordered. The average atomic ratios from EDX are consistent with $K_{0.88(6)}Fe_{1.63(4)}S_{2.00(1)}$, indicating that there are both potassium and iron deficiencies from ideal 122 stoichiometry, in good agreement with XRD fitting results. It should be noted that 18.5% of the iron precipitates on the surface of the ingot on cooling. The iron precipitates are easy to remove and have no influence on the physical properties of $K_xFe_{2-y}S_2$.

The in-plane resistivity $\rho_{ab}(T)$ of the $K_xFe_{2-y}S_2$ single crystal rapidly increases with decreasing the temperature

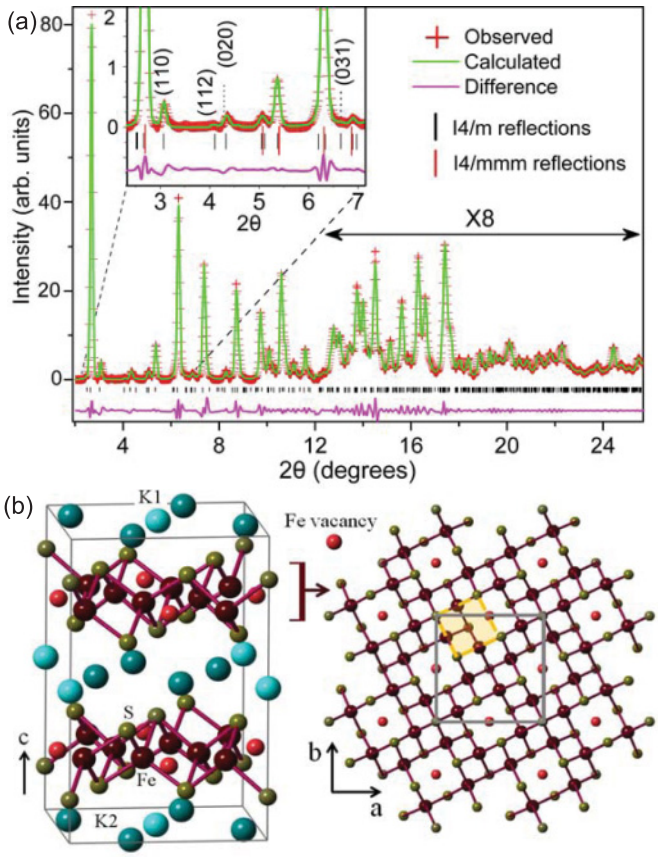

FIG. 1. (Color online) (a) Powder XRD patterns of $K_xFe_{2-y}S_2$ and fit using I4/m model. Inset: low-scattering-angle part, emphasizing the presence of superlattice reflections characteristic of I4/m symmetry. Enlarged isotropic thermal parameters, particularly in the potassium layer, are indicative of local disorder present in the structure. (b) Crystal structure of $K_xFe_{2-y}S_2$ in I4/m unit cell with vacant Fe1 sites (small red circle) and K1 sites (light blue) (left). Sketch of the FeS slab (c-axis view) with ordered Fe vacancies (right). Small yellow and large gray squares illustrate I4/mmm and I4/m unit cells, respectively.

from $\rho_{ab}(300\ \mathrm{K}) \sim 100\ \mathrm{m\Omega\ cm}$ and there is no obvious magnetoresistance (Fig. 2). The $\rho_{ab}(T)$ is thermally activated: $\rho = \rho_0 \exp(E_a/k_BT)$, where ρ_0 is a prefactor and k_B is the Boltzmann constant [inset (b) of Fig. 2]. Using the $\rho_{ab}(T)$ data from 70 to 300 K, we estimate $\rho_0 \sim 11.7(2)$ mΩ cm and the activation energy $E_a = 51.8(2)$ meV. The semiconducting behavior might be at least partially ascribed to the deficiency of Fe in the Fe-Se plane that would introduce a random scattering potential, just like in highly Fe deficient $K_xFe_{2-y}Se_2$ and $TlFe_{2-x}Se_2$.[13,14,19]

The magnetic susceptibility with $H\|ab$ is larger than with $H\|c$ [Fig. 3(a)], similar to the observed anisotropy in $TlFe_{2-x}Se_2$.[14] The most interesting characteristics are the absence of Curie-Weiss behavior and the obvious bifurcation between the zero-field-cooling (ZFC) and field-cooling (FC) curves below 32 K. This might suggest the presence of low-dimensional short-range magnetic correlations and/or a long-range magnetic order above 300 K, and an antiferromagnetic phase transition at low temperatures. The $M(T)$ irreversible behavior below 32 K implies some ferromagnetic contribution

TABLE I. Structural parameters for $K_xFe_{2-y}S_2$ at room temperature.[a]

Chemical formula	$K_{0.88}Fe_{1.63}S_2$
Space group	I4/m
a (Å)	8.3984(5)
c (Å)	13.5988(11)
V (Å^3)	959.17(11)

Interatomic distance (Å)		Bond angle (deg)	
$d_{Fe1\text{-}S2}$ [4]	2.4170(12)	S2-Fe1-S2 [2]	110.1(5)
$d_{Fe1\text{-}Fe2}$ [4]	2.5914(16)	S2-Fe1-S2 [4]	109.2(3)
$d_{Fe2\text{-}S1}$ [1]	2.3647(11)	S1-Fe2-S2 [1]	103.9(5)
$d_{Fe2\text{-}S2}$ [1]	2.3369(11)	S1-Fe2-S2 [1]	109.8(3)
$d_{Fe2\text{-}S2}$ [1]	2.3005(11)	S1-Fe2-S2 [1]	111.0(3)
$d_{Fe2\text{-}S2}$ [1]	2.2660(11)	S2-Fe2-S2 [1]	105.3(3)
$d_{Fe2\text{-}Fe2}$ [2]	2.6495(16)	S2-Fe2-S2 [1]	117.7(2)
$d_{Fe2\text{-}Fe2}$ [1]	2.8135(17)	S2-Fe2-S2 [1]	108.7(5)

Anion heights (Å)			
S1 to Fe1	1.388(5)	S2 to Fe1	1.384(5)
S1 to Fe2	1.334(5)	S2 to Fe2	1.439(5)

Atom	x	y	z	Occ	U_{iso} (Å^2)
K1	0	0	0.5	0.84(12)	0.059(15)
K2	0.80(2)	0.418(6)	0.5000	0.89(3)	0.059(15)
Fe1	0	0.5	0.25	0.08(4)	0.0136(3)
Fe2	0.2954(5)	0.4111(5)	0.2460(16)	1.00(1)	0.0136(3)
S1	0	0	0.1479(5)	1.00(0)	0.0111(6)
S2	0.1113(4)	0.292(1)	0.3518(3)	1.00(0)	0.0111(6)

[a]Values in brackets give the number of equivalent distances or angles of each type.

to magnetic susceptibility or a glassy transition where spins would be frozen randomly below the freezing temperature T_f. Similar magnetization was reported in $TlFe_{2-x}Se_2$ and

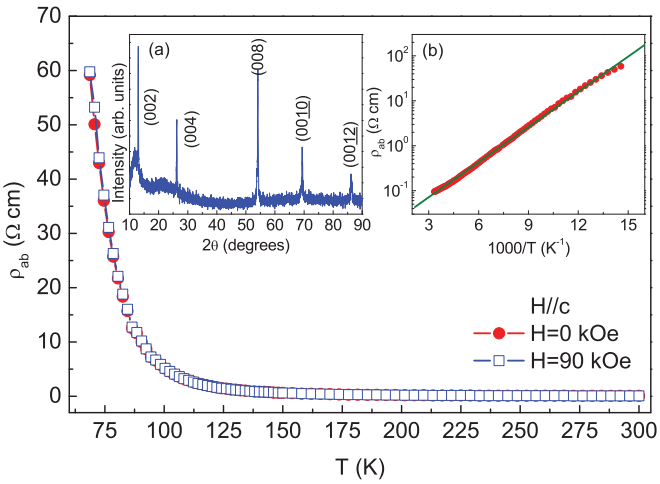

FIG. 2. (Color online) Temperature dependence of the in-plane resistivity $\rho_{ab}(T)$ with $H = 0$ [solid (red) circles] and 90 kOe [open (blue) squares]. Inset (a): single-crystal XRD pattern of $K_xFe_{2-y}S_2$ obtained using Rigaku Miniflex. The crystal surface is normal to the c axis with the plate-shaped surface parallel to the ab plane. Inset (b): fitting result using thermally activated model for $\rho_{ab}(T)$ in zero field.

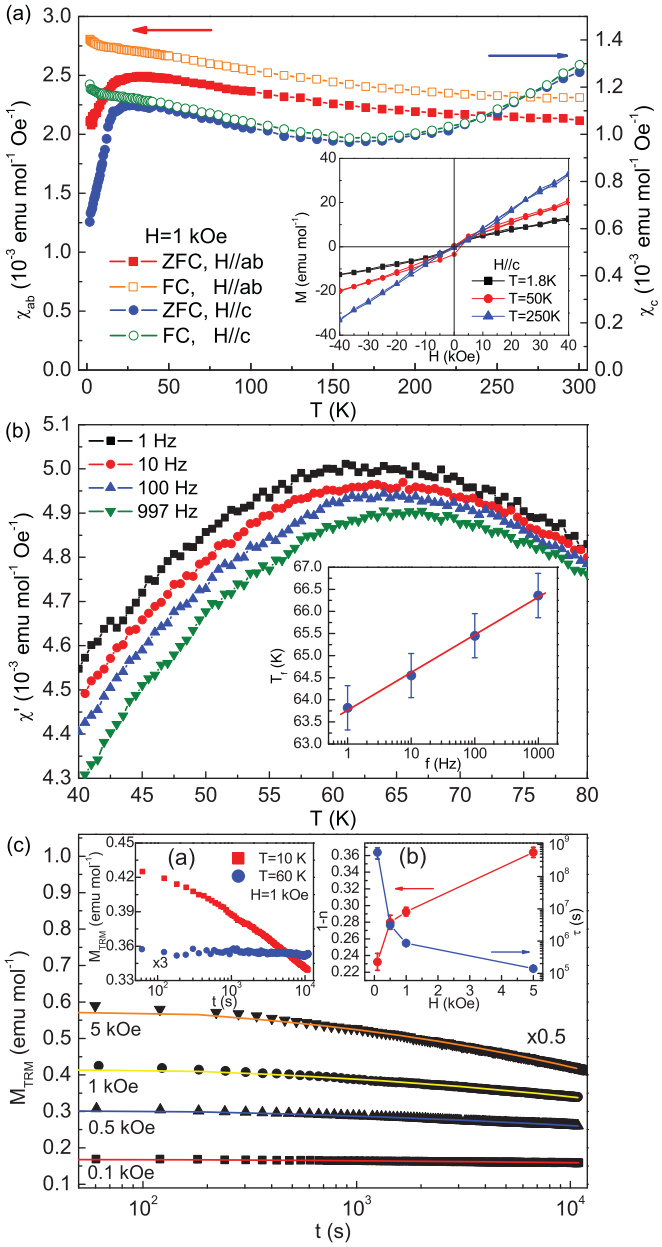

FIG. 3. (Color online) (a) ZFC and FC dc magnetic susceptibility with $H\|c$ and $H\|ab$ below 300 K. Inset: isothermal $M(H)$ for $H\|c$ at $T = 1.8$, 50, and 250 K. (b) Temperature dependence of $\chi'(T)$ measured at several fixed frequencies. Inset: frequency dependence of T_f. The solid line is the linear fit to the T_f data. (c) $M_{\rm TRM}$ vs t at 10 K with various dc fields and $t_w = 100$ s. The solid lines are fits using a stretched exponential function. Inset (a): $M_{\rm TRM}$ vs t at 10 and 60 K with $H = 1$ kOe and $t_w = 100$ s. Inset (b): magnetic field dependence of $1 - n$ and τ.

$KFeCuS_2$. [14,20] The inset in Fig. 3(a) shows the magnetization loops for $H\|c$. At 250 K, the M-H loop is almost linear and there is no hysteresis. However, an S-shaped M-H loop can be observed at 1.8 K, which is typical behavior of a SG system.[14] The S-shaped M-H loop is present at $T = 50$ K, which indicates that short-range ferromagnetic interaction may exist above T_f. As shown in Fig. 3(b), the peak in the real part of ac susceptibility $\chi'(T)$ exhibits strong frequency dependence in an ac magnetic field. When the frequency increases, the peak positions shift to higher temperatures whereas the magnitudes decrease, indicating typical SG behavior.[21] By fitting the frequency dependence of the peak shift using $K = \Delta T_f/(T_f \Delta \log f)$, we obtained $K = 0.0134(5)$ [inset of Fig. 3(b)]. This is in agreement with values ($0.0045 \leqslant K \leqslant 0.08$) found in the canonical SG system, but much smaller than in a typical superparamagnet.[21] Figure 3(c) shows the magnetic field dependence of the thermoremanent magnetization (TRM). The sample was cooled from $T = 60$ K (above T_f) in a magnetic field to $T = 10$ K (below T_f) and then kept at 10 K for $t_w = 100$ s. Then the magnetic field was removed and the magnetization decay $M_{\rm TRM}(t)$ was measured. It can be seen that, below T_f ($T = 10$ K), $M_{\rm TRM}(t)$ decays slowly so its value is nonzero even after several hours. This is another signature of the SG behavior, i.e., the existence of extremely slow spin relaxation below T_f.[21] In contrast, above T_f, $M_{\rm TRM}(t)$ quickly relaxes and does not show slow decay [inset (a) of Fig. 3(c)]. The magnetization decay can be explained well using a stretched exponential function commonly used to explain TRM behavior in SG systems, $M_{\rm TRM}(t) = M_0 \exp[-(t/\tau)^{1-n}]$, where M_0, τ, and $1 - n$ are the glassy component, the relaxation characteristic time, and the critical exponent, respectively. It can be seen [inset (b) of Fig. 3(c)] that τ decreases significantly with field but $1 - n$ increases slightly. On the other hand, the value of $1 - n$ is close to 1/3, consistent with theoretical predictions and the experiments on traditional SG systems.[22,23] The SG behavior could originate from Fe clusters induced by vacancies and disorder, and the exchange interactions between spins within a cluster would depend on the distribution of iron ions (Table I).[20] Indeed, in $TlFe_{2-x}Se_2$, the ground state is a reentrant spin glass if the content of Fe is less than 1.7.[14] However, for x values larger than 1.7, $TlFe_{2-x}Se_2$ becomes a superconductor below 20 K.[13] Therefore, superconductivity in $K_xFe_{2-y}S_2$ might be induced for a smaller deficiency of Fe.

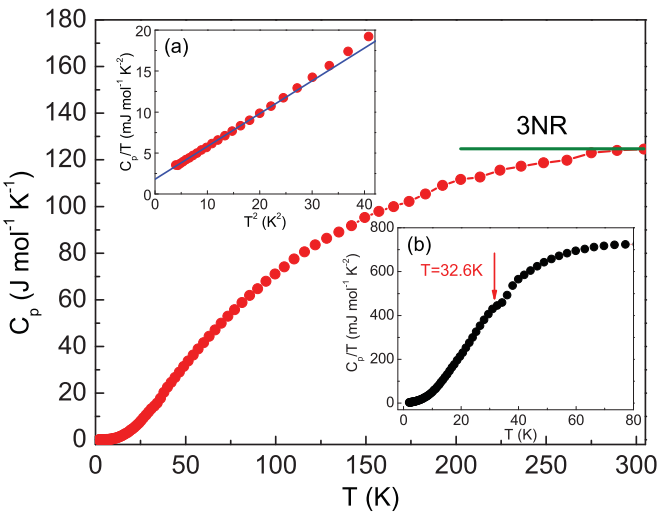

FIG. 4. (Color online) Temperature dependence of specific heat. Inset (a): low-temperature specific-heat data in the plot of C_p/T vs T^2. The solid (blue) line is the fitting curve using the formula $C_p/T = \gamma_{\rm SG} + \beta T^2$. Inset (b): enlarged area near the magnetic transition region of $C_p/T - T$.

The specific heat of $K_xFe_{2-y}S_2$ (Fig. 4) approaches the Dulong-Petit value of $3NR$ at high temperature, where N is the atomic number in the chemical formula ($N = 5$) and R is the gas constant. At low temperature, the specific heat can be fitted using $C_p = \gamma_{SG}T + \beta T^3$ [inset (a) of Fig. 4]. The variable γ_{SG} is commonly found in magnetic insulating SG systems, implying a constant density of states of the low-temperature magnetic excitations.[24–26] The second term is due to phonon contribution. The obtained γ_{SG} is 1.58(6) mJ mol^{-1} K^{-2}. The Debye temperatures Θ_D can be calculated from β through $\Theta_D = (12\pi^4 NR/5\beta)^{1/3}$ to be $\Theta_D = 284.3(7)$ K. It should be noted that, as opposed to the usual λ anomaly, there is a very weak broad hump of C_p/T near $T = 32.6$ K [inset (b) of Fig. 4]. This is expected for bulk low-dimensional or glassy magnetic systems.[24,27,28]

The discovery of $K_xFe_{2-y}S_2$ implies that it is possible to tune conductivity and magnetism by changing chalcogen elements (S and Se) in isostructural $K_xFe_{2-y}Ch_2$ materials. According to Table I, anion heights S1 to Fe1 and S1 to Fe2 in $K_{0.88(6)}Fe_{1.63(4)}S_{2.00(1)}$ are close to the alleged optimal value of 1.38 Å, comparable to distances in FePn-1111-type materials and lower than in $K_xFe_{2-y}Se_2$.[8,12] Hence, if the anion height is the crucial parameter, the sulfide compound should be a superconductor with higher T_c than that of $K_xFe_{2-y}Se_2$. However, it is a semiconductor, not a superconductor. We also note that in $K_xFe_{2-y}S_2$ there are two Fe sites and two corresponding anion heights. Our results indicate that the anion height values may be not essential parameters that govern superconductivity in AFeSe-122 compounds. In contrast, it suggests that disorder and site occupancies are significantly important.

In summary, we report the discovery of $K_xFe_{2-y}S_2$ single crystals isostructural to $T_c = 33$ K superconductor $K_xFe_{2-y}Se_2$ and exhibiting a similar width of formation and vacancies at both potassium and iron sites. Sulfide material is semiconducting and glassy magnetic, suggesting that the physical properties are governed by stoichiometry, defects, and local environment of Fe-S tetrahedra.

We thank S. L. Bud'ko for discussions, John Warren for help with scanning electron microscopy measurements, and John Hanson for help in facilitating the X7B experiment. The work at Brookhaven is supported by the US Department of Energy (DOE) under Contract No. DE-AC02-98CH10886 and in part by the Center for Emergent Superconductivity, an Energy Frontier Research Center funded by the DOE Office for Basic Energy Science.

[1] Y. Kamihara, T. Watanabe, M. Hirano, and H. Hosono, J. Am. Chem. Soc. **130**, 3296 (2008).
[2] M. Rotter, M. Tegel, and D. Johrendt, Phys. Rev. Lett. **101**, 107006 (2008).
[3] X. C. Wang, Q. Q. Liu, Y. X. Lv, W. B. Gao, L. X. Yang, R. C. Yu, F. Y. Li, and C. Q. Jin, Solid State Commun. **148**, 538 (2008).
[4] F. C. Hsu, J. Y. Luo, K. W. Yeh, T. K. Chen, T. W. Huang, P. M. Wu, Y. C. Lee, Y. L. Huang, Y. Y. Chu, D. C. Yan, and M. K. Wu, Proc. Natl. Acad. Sci. USA **105**, 14262 (2008).
[5] A. Subedi, L. Zhang, D. J. Singh, and M. H. Du, Phys. Rev. B **78**, 134514 (2008).
[6] Y. Mizuguchi, F. Tomioka, S. Tsuda, T. Yamaguchi, and Y. Takano, Appl. Phys. Lett. **93**, 152505 (2008).
[7] S. Medvedev, T. M. McQueen, I. Trojan, T. Palasyuk, M. I. Eremets, R. J. Cava, S. Naghavi, F. Casper, V. Ksenofontov, G. Wortmann, and C. Felser, Nat. Mater. **8**, 630 (2009).
[8] Y. Mizuguchi, Y. Hara, K. Deguchi, S. Tsuda, T. Yamaguchi, K. Takeda, H. Kotegawa, H. Tou, and Y. Takano, Supercond. Sci. Technol. **23**, 054013 (2010).
[9] A. Bill, H. Morawitz, and V. Z. Kresin, Phys. Rev. B **68**, 144519 (2003).
[10] J. Guo, S. Jin, G. Wang, S. Wang, K. Zhu, T. Zhou, M. He, and X. Chen, Phys. Rev. B **82**, 180520(R) (2010).
[11] A. F. Wang, J. J. Ying, Y. J. Yan, R. H. Liu, X. G. Luo, Z. Y. Li, X. F. Wang, M. Zhang, G. J. Ye, P. Cheng, Z. J. Xiang, and X. H. Chen, Phys. Rev. B **83**, 060512(R) (2011).
[12] A. Krzton-Maziopa, Z. Shermadini, E. Pomjakushina, V. Pomjakushin, M. Bendele, A. Amato, R. Khasanov, H. Luetkens, and K. Conder, J. Phys. Condens. Matter **23**, 052203 (2011).
[13] M. H. Fang, H. D. Wang, C. H. Dong, Z. J. Li, C. M. Feng, J. Chen, and H. Q. Yuan, Europhys. Lett. **94**, 27009 (2011).
[14] J. J. Ying, A. F. Wang, Z. J. Xiang, X. G. Luo, R. H. Liu, X. F. Wang, Y. J. Yan, M. Zhang, G. J. Ye, P. Cheng, and X. H. Chen, e-print arXiv:1012.2929.
[15] K. Kihou, T. Saito, S. Ishida, M. Nakajima, Y. Tomioka, H. Fukazawa, Y. Kohori, T. Ito, S. Uchida, A. Iyo, C. Lee, and H. Eisaki, J. Phys. Soc. Jpn. **79**, 124713 (2010).
[16] A. C. Larson and R. B. Von Dreele, Los Alamos National Laboratory Report No. LAUR 86-748, 1994.
[17] B. H. Toby, J. Appl. Crystallogr. **34**, 210 (2001).
[18] W. Bao, Q. Huang, G. F. Chen, M. A. Green, D. M. Wang, J. B. He, X. Q. Wang, and Y. Qiu, e-print arXiv:1102.0830.
[19] D. M. Wang, J. B. He, T.-L. Xia, and G. F. Chen, Phys. Rev. B **83**, 132502 (2011).
[20] M. Oledzka, K. V. Ramanujachary, and M. Greenblatt, Mater. Res. Bull. **31**, 1491 (1996).
[21] J. A. Mydosh, *Spin Glasses: An Experimental Introduction* (Taylor & Francis, London, 1993).
[22] I. A. Campbell, Phys. Rev. B **37**, 9800 (1988).
[23] D. Chu, G. G. Kenning, and R. Orbach, Phys. Rev. Lett. **72**, 3270 (1994).
[24] C. Y. Huang, J. Magn. Magn. Mater. **51**, 1 (1985).
[25] D. Meschede, F. Steglich, W. Felsch, H. Maletta, and W. Zinn, Phys. Rev. Lett. **44**, 102 (1980).
[26] N. P. Raju, E. Gmelin, and R. K. Kremer, Phys. Rev. B **46**, 5405 (1992).
[27] G. E. Brodale, R. A. Fisher, W. E. Fogle, N. E. Phillips, and J. van Curen, J. Magn. Magn. Mater. **31–34**, 1331 (1983).
[28] L. O.-S. Martin, J. P. Chapman, L. Lezama, J. J. S. Garitaonandia, J. S. Marcos, J. Rodríguez-Fernández, M. I. Arriortua, and T. Rojo, J. Mater. Chem. **16**, 66 (2006).